Yang, J. & Liu, X. (2016). *Géotechnique* **66**, No. 6, 500–514 [http://dx.doi.org/10.1680/jgeot.15.P.205]

Shear wave velocity and stiffness of sand: the role of non-plastic fines

J. YANG* and X. LIU*

Current knowledge on the shear wave velocity (V_s) and associated stiffness (G_0) of sand is built mainly on the results of extensive laboratory studies on clean quartz sands. Often natural sands are not clean, but contain a certain amount of fines. The role of fines in altering the stiffness of sands is a matter of great concern, yet remains poorly understood. This paper presents an investigation into the problem through well-controlled laboratory experiments in conjunction with analysis and interpretation at the macro and micro scale. The laboratory experiments were conducted for a sequence of mixtures of clean quartz sand and crushed silica fines under saturated conditions, by the simultaneous use of the resonant column (RC) and bender element (BE) techniques. A broad range of states in terms of void ratio, confining stress and fines content was covered so as to obtain a comprehensive view on the effect of fines and the possible interplay with other factors. Both the RC and BE tests showed that G_0 tends to decrease continuously as the quantity of fines is increased and the reduction rates are similar; a similar stress dependence is also obtained for G_0 from both types of testing. Nevertheless, G_0 values obtained from BE tests are notably greater than those obtained from RC tests, and this effect of testing method is shown to be coupled with the sample reconstitution method. A new approach that allows unified characterisation of G_0 values for both clean sand and sand–fines mixtures is developed in a sound theoretical framework, thereby providing important insights into the various empirical correlations that involve G_0 (or V_s) in geotechnical engineering practice. A new micro-scale mechanism is also suggested for the observed effect of fines, which attributes the reduction of G_0 caused by fines to the decrease in the coordination number at an approximately constant void ratio.

KEYWORDS: dynamics; elasticity; laboratory tests; sands; stiffness

INTRODUCTION

The characterisation of shear wave velocity (V_s) and associated small-strain stiffness (G_0) for granular soils has been a subject of long-standing interest in soil mechanics and geotechnical engineering (Stokoe *et al.*, 1999; Clayton, 2011). A sound knowledge has been developed over the last several decades, mainly through well-controlled laboratory experiments on clean, uniform, quartz sands (e.g. Hardin & Richart, 1963; Hardin & Drnevich, 1972; Iwasaki & Tatsuoka, 1977; Seed *et al.*, 1986; Lo Presti *et al.*, 1997; Kuwano *et al.*, 2000; Youn *et al.*, 2008; Wichtmann & Triantafyllidis, 2009; Gu *et al.*, 2015; and the references therein). Among the various factors that may affect the stiffness property, void ratio and confining stress are recognised to be the most important ones, and several empirical equations accounting for the two factors are now commonly used in practice and in the development of constitutive models (Ishihara, 1996; Taiebat & Dafalias, 2008). These empirical equations often take a general form as follows

$$G_0 = AF(e)\left(\frac{\sigma'}{p_a}\right)^n \quad (1)$$

where σ' is the mean effective stress; p_a is a reference stress, usually taken as the atmospheric pressure; $F(e)$ is a function of the void ratio e; and A and n are two best-fit parameters. The exponent n has received much discussion in the past (e.g. Goddard, 1990; Chang *et al.*, 1991; McDowell & Bolton, 2001); it reflects the contact conditions at the grain scale and takes the value of 1/3 from the classical Hertz–Mindlin contact theory. The measured values, however, typically range between 0·35 and 0·6 for sands, and for simplicity the value of 0·5 is commonly adopted in empirical equations (Hicher, 1996; Ishihara, 1996).

Often natural sands are not clean, but contain a certain amount of fines (< 63 μm). A number of experimental studies have shown that the presence of fines can alter the large-strain shear behaviour of clean sands under either monotonic or cyclic loading conditions (e.g. Lade & Yamamuro, 1997; Polito & Martin, 2001; Thevanayagam *et al.*, 2002). A concrete example is given in Fig. 1, which shows that the liquefaction susceptibility of saturated Toyoura sand can be significantly enhanced by the addition of non-plastic silica fines (Yang & Wei, 2012). Concerns have been raised over such issues as what impact fines have on the shear wave velocity and the associated stiffness of sands, and whether the empirical equations developed from experiments on clean sands are applicable for sands with fines. In the current literature, however, available studies addressing these issues are limited compared with the enormous body of studies on clean sands.

Recent notable work on the effect of fines includes that by Wichtmann *et al.* (2015), who conducted a structured resonant column testing programme on a quartz sand mixed with a non-plastic quartz powder of varying quantities (0–20% by mass). The study showed that the small-strain stiffness (G_0) decreased with increasing fines content (FC) up to about 10%, but a further increase of FC to 20% did not cause measurable changes in G_0. This result is not in full agreement with that of Salgado *et al.* (2000), which was derived from laboratory experiments on Ottawa sand

Manuscript received 13 September 2015; revised manuscript accepted 13 January 2016. Published online ahead of print 17 February 2016.
Discussion on this paper closes on 1 November 2016, for further details see p. ii.
* Department of Civil Engineering, The University of Hong Kong, Hong Kong.

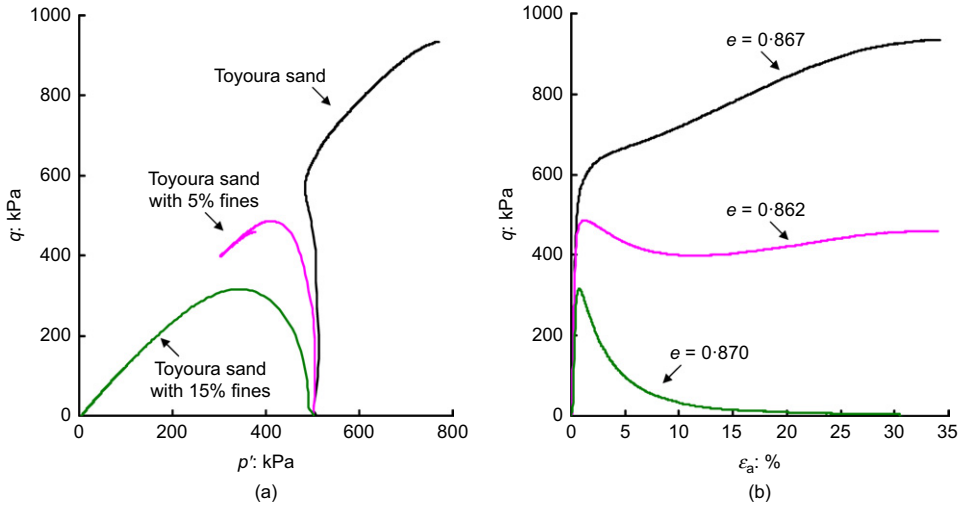

Fig. 1. Experimental evidence for changes in the liquefaction potential of sand caused by the addition of fines: (a) q–p' response in triaxial space; (b) q–ε_a response

mixed with non-plastic silica fines (FC = 0–20%) by using piezoceramic bender elements in a triaxial device. Those experiments showed that the value of G_0 continuously decreased with an increase of FC up to 20% and became as low as 40% of the clean sand at the highest FC; a dramatic variation of the stress exponent n was also measured, ranging from 0·435 at FC = 0 to 0·809 at FC = 20%. Given that both Ottawa sand and silica fines are hard grained materials and given the range of confining pressure applied, the value of 0·809 appears to be unusually high compared with the reported values in the literature. Moreover, a dramatic variation in the stress exponent does not appear to be in agreement with the observations of Iwasaki & Tatsuoka (1977) and Chien & Oh (2002) that the stress exponent is insensitive to the presence of fines.

The experimental data from previous studies provide a useful reference for understanding the effect of fines. Nevertheless, the diverse observations indicate that the problem remains highly complex and not yet fully understood. Previous studies have often involved different materials (in terms of grain shape, size distribution and mineralogy) and different testing methods, making it difficult to evaluate the discrepancies through direct comparison. For example, the bender element (BE) tests of Salgado *et al.* (2000) were performed on saturated specimens prepared by slurry deposition, whereas the resonant column (RC) tests of Wichtmann *et al.* (2015) were conducted on dry specimens prepared by air pluviation. Several studies (e.g. Nakagawa *et al.*, 1997) have shown that under otherwise similar conditions, G_0 values measured on dry specimens are not, as usually assumed, exactly the same as those of saturated specimens. In particular, the presence of fines raises a concern about the effect of grain segregation in the deposition process and a concern about the effect of grain size ratio.

Unlike the widely recognised technique of RC testing, BE testing is not yet standardised worldwide, partly because of the variability of results (e.g. Jovicic *et al.*, 1996; Lee & Santamarina, 2005; Yamashita *et al.*, 2009). The variability is mainly associated with the determination of the travel time of shear waves. As demonstrated by Yamashita *et al.* (2009) and Yang & Gu (2013), even for uniform clean sand and glass beads, significantly different travel times and consequently different V_s and G_0 values may be derived when signals are not properly interpreted. It may therefore be speculated that the observed discrepancies on the effect of fines might be caused by the uncertainty in signal interpretation or attributable to the effect of testing methods. However, the literature is lacking solid data showing how the presence of fines affects the shear wave signals in sand specimens and whether considerable uncertainty tends to emerge when fines are present. Systematic data sets are needed that allow a meaningful comparison of BE and RC measurements on sand–fines mixtures and at the same time can serve as a useful reference in the validation and calibration of numerical simulations and theoretical developments in this important realm.

With the aim of addressing the above concerns, a specifically designed experimental programme has been carried out using an apparatus that incorporates both RC and BE functions. The apparatus allows RC and BE testing to be performed on an identical specimen, thus affording a more reliable and convincing comparison. All specimens were tested under the saturated rather than the dry condition, because the former is more relevant to practical situations. To obtain a comprehensive view on the effect of fines and the possible interplay with other factors, the experimental programme covered a wide range of conditions in terms of void ratio, confining stress and fines content. This paper presents the main results along with a detailed discussion and interpretation from the macro-scale and micro-scale perspectives. A new approach is put forward that allows unified characterisation of G_0 values for both clean sand and sand–fines mixtures in a theoretical framework, and a micro-scale mechanism is also suggested to explain the observed effect of fines.

TEST MATERIALS AND METHODS

In the laboratory experiments Toyoura sand was used as the base sand and crushed silica fines were used as the additive. Using artificially created mixtures allows good control of grain characteristics and facilitates experimental repeatability so that any more complex effects or uncertainties are eliminated. Table 1 gives the basic physical properties of the two materials, and Fig. 2 shows their particle size distribution curves together with microscopy images. Toyoura sand is a uniform quartz sand with sub-angular to sub-rounded grains, whereas the crushed silica fines are composed of non-plastic angular grains. To produce a sequence of sand–fines mixtures, the quantity of crushed silica fines was varied from 0 to 30% by mass. The threshold

Table 1. Basic properties of test materials

Material	G_s	D_{10}: μm	D_{50}: μm	D_{60}: μm	C_u
Toyoura sand	2·65	166·0	216·0	231·0	1·392
Silica fines	2·64	27·5	54·0	60·0	2·182

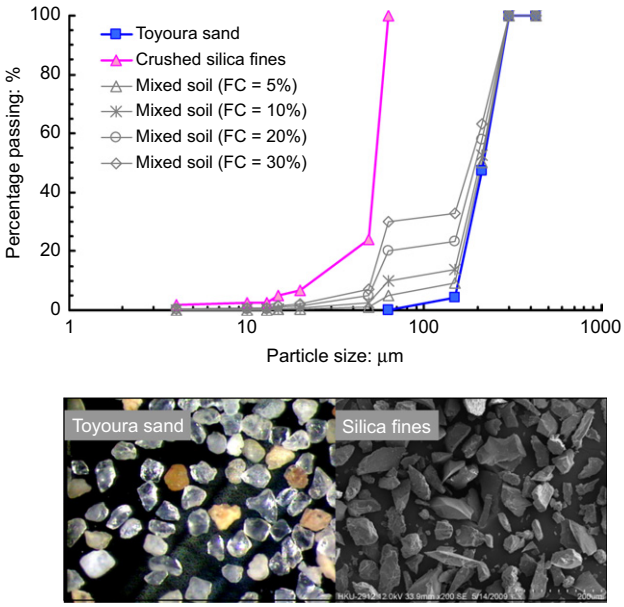

Fig. 2. Particle size distribution curves and microscopic images of tested materials

fines content beyond which the mixture tended to be fines-dominated (i.e. the load-carrying frame being primarily formed by fine grains, see Thevanayagam *et al.* (2002)) was quantified to be about 40%; hence all mixtures in the study were sand-dominated.

The apparatus used in the study has both RC and BE features and a robust signal conditioning and data acquisition system, as shown in Fig. 3. It can accommodate a soil specimen 50 mm in diameter and 100 mm high, with an air-filled cell pressure up to 1 MPa. The resonant column is of bottom-fixed and top-free configuration which, compared with the free–free configuration, has the advantages of high available torque and convenient access to the specimen for effective stress control. A pair of piezoceramic bender/-extender elements is set in the top cap and base pedestal as the transmitter and receiver, respectively. The bender elements are used to generate shear waves that propagate vertically with horizontal polarisation, while the extender elements are used to generate compression waves. A careful calibration of the apparatus has been carried out for both RC and BE functions (Yang & Gu, 2013): for the former a set of aluminium bars of different dimensions was used to establish a calibration curve for the frequency-dependent mass polar moment of inertia of the drive head, whereas for the latter the calibration was conducted to determine the system delay, including the response time of the bender elements and the travel time in the cables, and to check the phase relationship between the input and output signals.

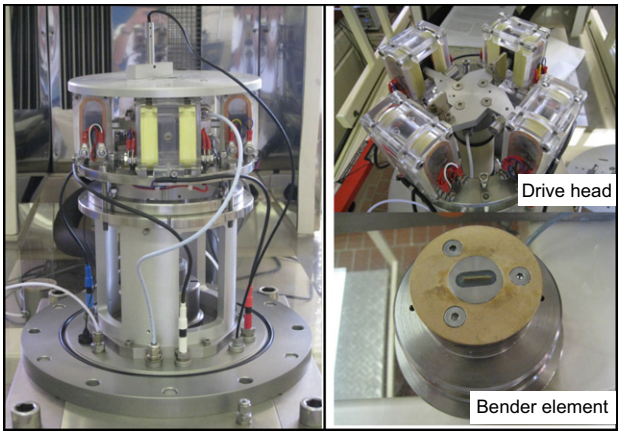

Fig. 3. Resonant column apparatus with piezoceramic bender elements installed

All specimens were prepared by the moist tamping method (Ishihara, 1996) in conjunction with the under-compaction technique (Ladd, 1978). This method was chosen because it can produce a very wide range of soil densities and has the advantage of preventing segregation and enhancing uniformity. As previous studies focused mainly on medium-dense and dense samples that would exhibit strain-hardening rather than contractive, liquefaction behaviour, the testing programme has purposely included a number of specimens in the loose state. All specimens were saturated in two stages: initially by flushing the specimen with carbon dioxide and de-aired water, and then by applying back pressure. Specimens with a Skempton B-value greater than 0·95 were considered saturated. After saturation, each specimen was subjected to an isotropic confining stress in stages, typically at 50, 100, 200, 400 and 500 kPa. When the specimen was brought to a specific confining pressure level, it was consolidated for about 15 min so that the reading of the internal linear variable differential transducer (LVDT) became stable and the volume change was measured; then the BE test was performed under a range of excitation frequencies. Following the BE test, the RC test was performed on the same specimen for the purpose of comparison of the stiffness measurements. The strain level involved in all tests was in the order of 10^{-5} or below. A summary of the testing series is given in Table 2.

RESULTS AND ANALYSIS

Measurements from BE tests

In each BE test a set of sinusoid signals at various frequencies (from 1 to 40 kHz) was used as the excitation, and the received signals were examined in a whole view to better identify the travel time of the shear wave. The signal corresponding to the excitation frequency of 10 kHz was found to consistently yield a clear arrival of the shear wave in both clean sand and mixed soil specimens. This is in good agreement with the observation of Yang & Gu (2013) on samples of uniform glass beads tested in the same apparatus. This result also agrees with the observation of Brignoli *et al.* (1996) from their pulse tests on uniform Ticino sand that the most interpretable waveforms typically occurred in the range of 3–10 kHz for specimens of 100–140 mm high. As an example, Fig. 4(a) shows a set of received signals in a clean sand specimen under a range of confining stresses, from as low as 50 kPa to as high as 500 kPa; for the purpose of comparison, Fig. 4(b) shows the received signals in a mixed specimen with 10% fines at a similar void ratio.

For either the clean sand specimen or the mixed soil specimen, the arrival of the shear wave can be clearly identified (marked by a downward solid triangle in each waveform). As the confining stress increased, the travel time of the shear wave decreased accordingly. A comparison of Figs 4(a) and 4(b) indicates that the waveforms in the mixed

Table 2. Summary of testing series (e = void ratio; σ' = effective confining stress (kPa))

Material	State 1 (e, σ')	State 2 (e, σ')	State 3 (e, σ')	State 4 (e, σ')	State 5 (e, σ')
Clean sand FC = 0%	(0·903,50)	(0·899,100)	(0·893,200)	(0·793,400)	(0·881,500)
	(0·805,50)	(0·802,100)	(0·798,200)	(0·842,400)	(0·791,500)
	(0·887,50)	(0·883,100)	(0·878,200)	—	(0·867,500)
	(0·859,50)	(0·855,100)	(0·850,200)	—	(0·839,500)
	(0·937,50)	(0·933,100)	(0·926,200)	—	(0·912,500)
	—	(0·856,100)	(0·851,200)	—	—
FC = 5%	(0·934,50)	(0·929,100)	(0·921,200)	—	(0·905,500)
	(0·802,50)	(0·800,100)	(0·796,200)	(0·790,400)	—
	(0·820,50)	(0·817,100)	(0·812,200)	(0·805,400)	(0·802,500)
	(0·905,50)	(0·901,100)	(0·894,200)	—	(0·882,500)
	(0·874,50)	(0·870,100)	(0·864,200)	(0·855,400)	(0·852,500)
FC = 10%	(0·815,50)	(0·811,100)	(0·806,200)	(0·794,400)	—
	(0·809,50)	(0·805,100)	(0·800,200)	(0·792,400)	(0·789,500)
	(0·874,50)	(0·870,100)	(0·863,200)	(0·853,400)	(0·848,500)
	(0·934,50)	(0·927,100)	(0·916,200)	—	(0·896,500)
	—	(0·863,100)	(0·858,200)	—	—
FC = 20%	(0·810,50)	(0·806,100)	(0·800,200)	(0·791,400)	(0·787,500)
	(0·813,50)	(0·809,100)	(0·803,200)	(0·794,400)	(0·790,500)
	(0·881,50)	(0·874,100)	(0·862,200)	(0·841,400)	(0·832,500)
	(0·936,50)	(0·925,100)	(0·910,200)	—	(0·881,500)
	(0·937,50)	(0·926,100)	(0·910,200)	(0·887,400)	(0·877,500)
FC = 30%	(0·810,50)	(0·805,100)	(0·799,200)	(0·788,400)	(0·783,500)
	(0·875,50)	(0·867,100)	(0·855,200)	(0·836,400)	—
	(0·865,50)	(0·858,100)	(0·848,200)	(0·831,400)	(0·824,500)
	(0·930,50)	(0·917,100)	(0·898,200)	—	(0·862,500)

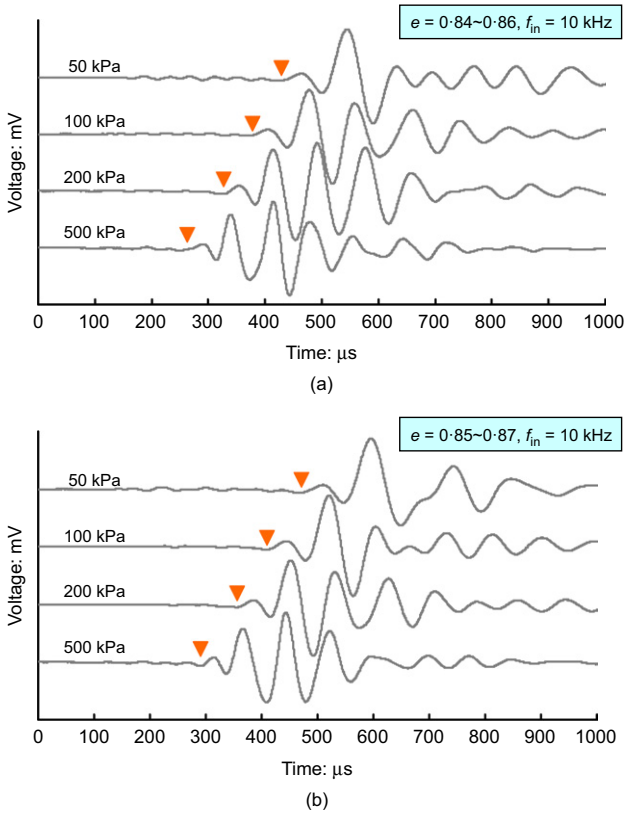

Fig. 4. Shear wave signals at various effective confining stresses: (a) clean sand specimen; (b) sand with 10% fines

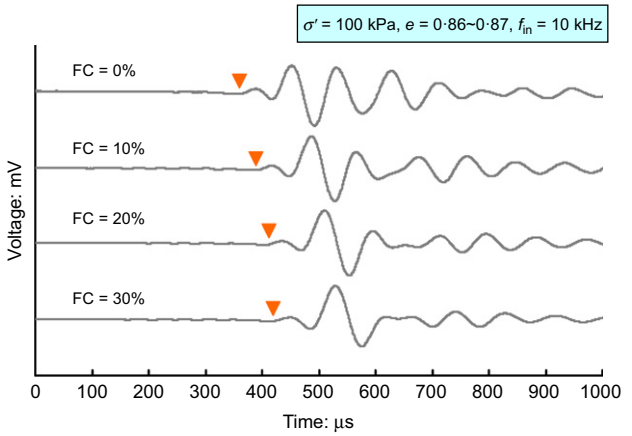

Fig. 5. Shear wave signals in saturated sand specimens with different percentages of fines

soil specimen are similar to their counterparts in the clean sand specimen, suggesting that the presence of fines would not introduce notable uncertainty in signal interpretation. Nevertheless, the presence of fines was found to increase the shear wave travel time. This effect can be observed more clearly in Fig. 5, where received signals in four specimens with different quantities of fines (FC = 0–30%) are compared. Note that all four specimens were carefully controlled to achieve a similar state (e = 0·86–0·87, σ' = 100 kPa) so as to afford a meaningful comparison.

A more comprehensive view of G_0 values measured under various conditions is given in Fig. 6, where G_0 values are shown as a function of void ratio for samples at different quantities of fines and at different confining pressures. It is clear from the plots that G_0 is dependent on void ratio, confining stress and the percentage of fines. Under otherwise similar conditions, G_0 increases with decreasing void ratio and with increasing confining stress, but it decreases with increasing fines content. A notable feature of the results in Fig. 6 is that the void ratio dependence of the sand–fines mixtures appears to be similar to that of clean sand, and this dependence seems to be insensitive to changes in

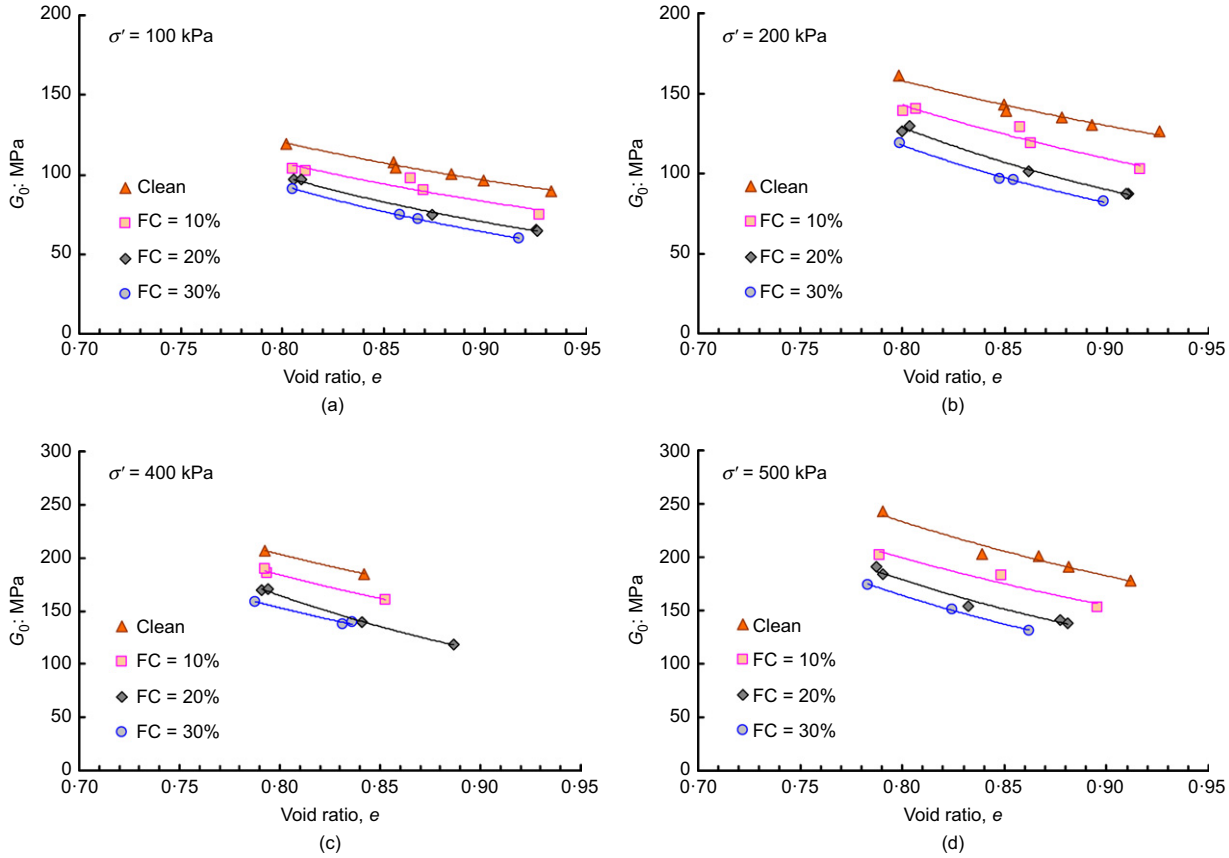

Fig. 6. Variation of shear modulus with void ratio at different percentages of fines (BE tests): (a) $\sigma' = 100$ kPa; (b) $\sigma' = 200$ kPa; (c) $\sigma' = 400$ kPa; (d) $\sigma' = 500$ kPa

confining stress. The state dependence of G_0 is of particular interest and will be discussed in more detail in sections that follow.

Comparison of BE and RC measurements

It is of interest to examine whether a similar effect of fines on V_s and G_0 can be obtained from RC tests. Fig. 7 shows an example of the frequency response of four specimens with different quantities of fines. All specimens were brought to a similar state ($e = 0{\cdot}85$–$0{\cdot}86$, $\sigma' = 200$ kPa) so that any observed difference can be attributed mainly to the effect of fines. Clearly, even a small amount of fines (FC = 5%) is able to cause a notable shift of the resonant frequency to the low frequency end, thus leading to a reduction of V_s and G_0 in accordance with the relations as follows

$$\begin{cases} \dfrac{I}{I_0} = \beta \tan \beta \\ \beta = \dfrac{2\pi f_n}{V_s} L \end{cases} \tag{2}$$

where f_n is the resonant frequency; I is the mass polar moment of inertial of the specimen and I_0 is the mass polar moment of inertia of the added mass; and L is the height of the specimen.

To facilitate comparison with BE measurements, G_0 values measured from RC tests are also presented as a function of void ratio for samples at various percentages of fines and confining stresses, as given in Fig. 8. By comparing the results in Figs 6 and 8, it is possible to conclude that both the BE and RC tests tend to yield a similar effect of fines and also that the void ratio dependence of G_0 obtained from both types of testing appears to be similar.

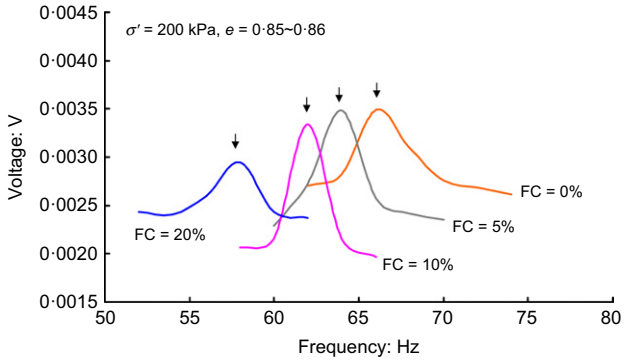

Fig. 7. Frequency response curves of saturated sand specimens with different percentages of fines

On the other hand, for a given specimen at a given state, the G_0 value measured by BE testing is notably greater than that measured by RC testing. For example, for a clean sand specimen at a confining pressure of 100 kPa and a void ratio of 0·802, the G_0 value obtained from BE testing is 118·6 MPa, which is approximately 20% larger than the RC measurement under the same state; meanwhile, for a mixed soil specimen (FC = 20%) at a confining pressure of 400 kPa and a void ratio of 0·791, the G_0 value measured by RC testing is 140·9 MPa, which is approximately 24% less than the BE measurement. This observation is interesting, and it warrants a further comparison of G_0 values obtained by all BE and RC tests, as given in Fig. 9, where RC test data are plotted against their BE counterparts and the diagonal line represents the equality line. Clearly, for either clean sand or sand–fines mixtures, G_0 values determined by BE tests are

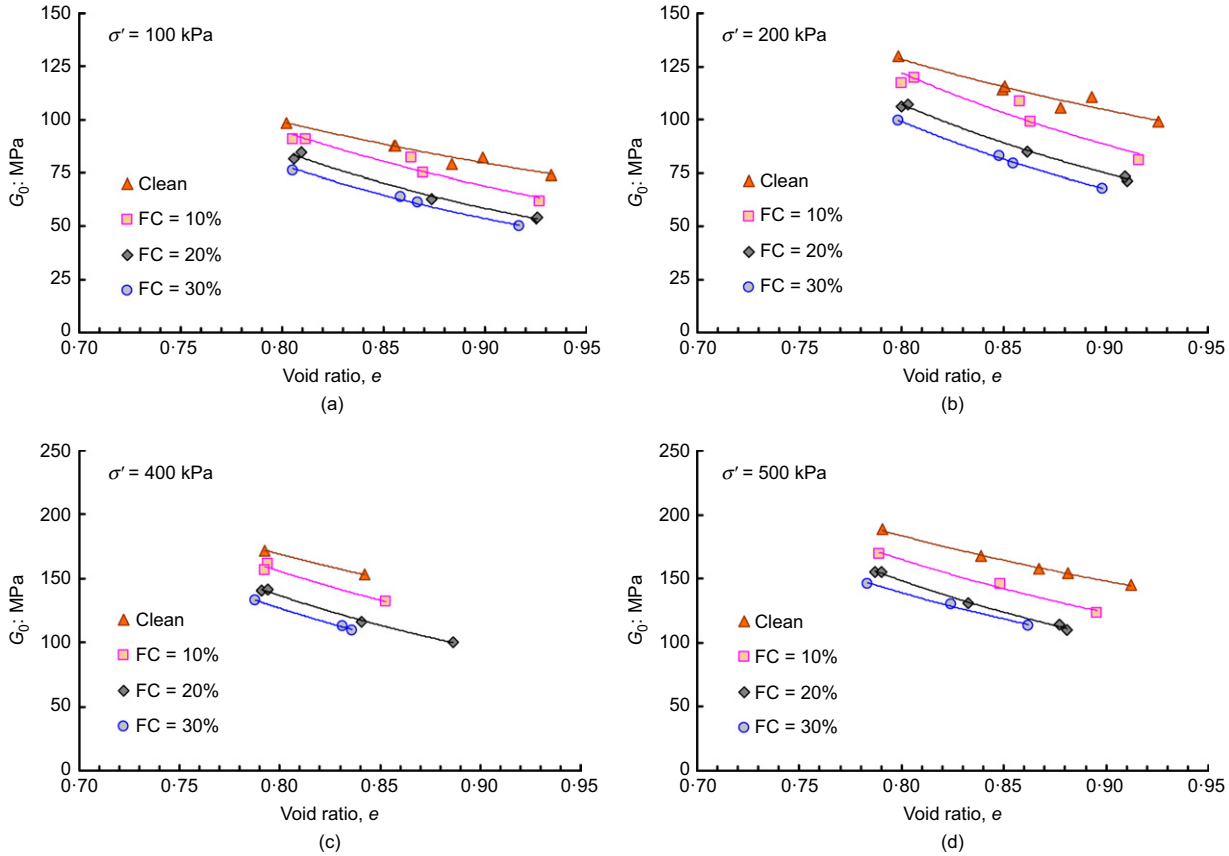

Fig. 8. Variation of shear modulus with void ratio at different percentages of fines (RC tests): (a) $\sigma' = 100$ kPa; (b) $\sigma' = 200$ kPa; (c) $\sigma' = 400$ kPa; (d) $\sigma' = 500$ kPa

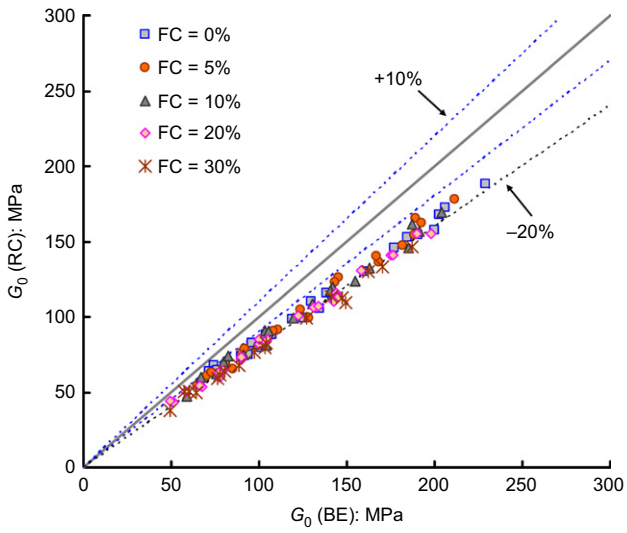

Fig. 9. Comparison of shear modulus measurements from resonant column and bender element tests

consistently larger than those from RC tests by approximately 20%. The possible reasons for this difference may include: (*a*) the strain level involved in BE tests is relatively lower than that involved in RC tests, and (*b*) the RC test measures the overall stiffness of a specimen, whereas the BE test measures the central part of the specimen between the transmitter and the receiver, which is likely to be stiffer than the whole specimen owing to the boundary effect.

The observed difference between BE and RC measurements is bigger than that obtained from testing uniform glass beads on the same apparatus (Yang & Gu, 2013). In that earlier study the difference was found to be within 10%, with BE measurements being slightly larger. This raises the question of what the possible reason is for the differing observations. All specimens of glass beads in the earlier study were prepared by dry tamping, whereas in the current study all specimens were prepared by moist tamping. One may therefore speculate that the effect of the testing method might be coupled with the sample preparation method. To verify this, a set of Toyoura sand specimens were prepared by dry tamping, then saturated and subjected to BE and RC testing using the same apparatus. The test results are shown in Fig. 10. The dry tamping method was not used to prepare specimens of mixtures to avoid uncertainty with the possible effect of segregation. It is striking to note that the BE and RC measurements become comparable for specimens prepared by dry tamping, with the former being slightly larger. The difference observed on Figs 9 and 10 is understandable if one recalls the effect of sample preparation that has been observed on the large-strain behaviour of sands (e.g. Miura & Toki, 1982; Sze & Yang, 2014). Generally, the dry tamping method tends to produce samples with an anisotropic fabric because of the gravitational deposition of grains, whereas samples produced by the moist tamping method tend to be more isotropic because of the capillary effect (Sze & Yang, 2014). A detailed discussion of the issue is beyond the scope of this paper, but further work along this line is worthwhile.

Effect of fines on G_0 *values*

Given that G_0 values are dependent on both confining stress and void ratio, it is important to take account of these two factors in quantifying the effect of fines. In doing so, for a

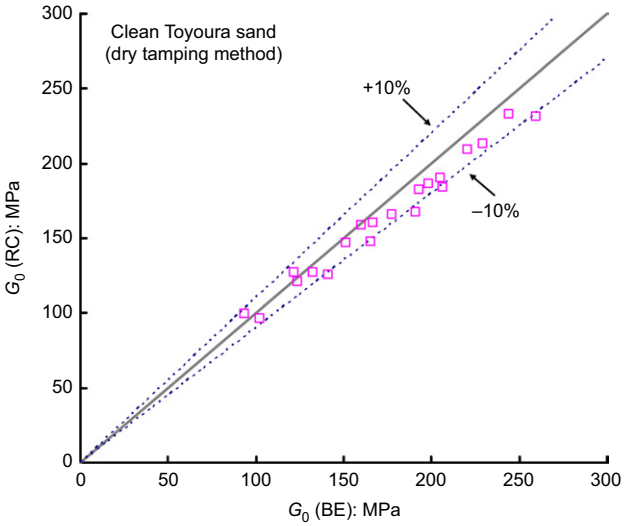

Fig. 10. Comparison of shear modulus measurements from RC and BE tests on dry-tamped clean sand samples

given confining stress the values of G_0 are first divided by a void ratio function $F(e)$ to remove the influence of void ratio, and then presented as a function of fines content, as shown in Fig. 11. For ease of comparison, RC test data are plotted in Fig. 11(a) and BE test data are plotted in Fig. 11(b). Although several void ratio functions are available in the literature, the following one has received wide recognition (Iwasaki & Tatsuoka, 1977; Yamashita *et al.*, 2009) and is adopted here

$$F(e) = \frac{(2{\cdot}17 - e)^2}{1 + e} \tag{3}$$

For either RC or BE tests, the void ratio-corrected G_0 values decrease approximately linearly with increasing fines content at a given confining stress. The rate of reduction at high confining stress tends to be slightly greater than that at low confining stress, but at a specific confining stress the reduction rate measured by RC tests appears to be similar to that measured by BE tests. It is worth noting that the observed reduction of G_0 caused by the addition of fines is not due to lower stiffness of the fines compared with the base sand. Laboratory experiments conducted on pure silica fines indicate that under otherwise similar conditions, the crushed silica fines have relatively higher stiffness than the base sand (see Table 3).

Furthermore, the void ratio-corrected G_0 values are plotted as a function of confining stress that is also normalised by a reference stress in Fig. 12. For the purpose of comparison, RC test data are presented in Fig. 12(a) and BE test data are given in Fig. 12(b). In each plot, the two trend lines represent the case of clean sand (upper bound) and the case of highest fines content tested (lower bound), and the range in between them indicates the effect of varying fines content. The stress dependence of G_0 is immediately evident in both plots, and this dependence can be represented by a power law as given in equation (1). For each case of fines content, the stress exponent n and the coefficient A can be determined by regression, and their values are summarised in Table 4. The high coefficients of determination suggest that the empirical equation with the void ratio function in equation (3) works reasonably well for both clean sand and sand–fines mixtures. In particular, the data obtained have several important features: (*a*) the stress exponent is not sensitive to the presence of fines; (*b*) the reduction of G_0 is mainly reflected by the coefficient A in the way that it decreases with increasing fines content; and (*c*) the BE and RC tests tend to yield a similar stress exponent.

By plotting values of A as a function of fines content, a fairly good correlation is obtained (Fig. 13). Using the RC data as an example, the correlation can be given in an exponential form as follows

$$A = 95{\cdot}39e^{-\mathrm{FC}} \tag{4}$$

where A is in MPa and FC is in decimal. Note that at FC = 0, the coefficient A takes the value for clean sand (Table 4). Combining equations (1), (3) and (4) yields a simple model for estimating G_0 values for clean sand and sand–fines mixtures. As an example, Fig. 14(a) shows the calculated G_0 values plotted against the measured ones from RC tests, indicating a reasonably good agreement between them.

The applicability of empirical equations developed from experiments on clean sands to sand–fines mixtures is an interesting concern. The classical Hardin's equation (Hardin & Richart, 1963; Hardin & Black, 1966) is one that is

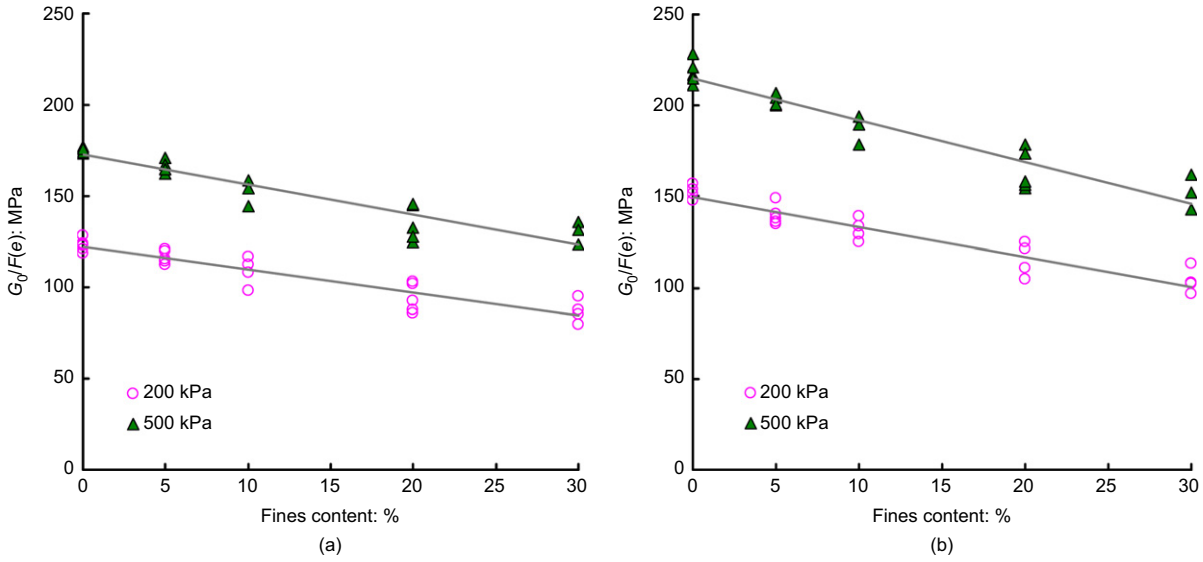

Fig. 11. Void ratio-corrected shear modulus as a function of fines content: (a) RC measurements; (b) BE measurements

Table 3. Comparison of G_0 values for silica fines and Toyoura sand

Testing method	$G_0/F(e)$: MPa*			
	Silica fines		Toyoura sand	
	$\sigma' = 100$: kPa	$\sigma' = 200$: kPa	$\sigma' = 100$: kPa	$\sigma' = 200$: kPa
RC	136·06	174·12	94·03	123·05
BE	155·14	199·28	113·55	151·60

*The void ratio-corrected G_0 value is an average.

commonly used as a first approximation to estimate G_0 values. For angular sands the equation is given as

$$G_0 = 3{\cdot}9\frac{(2{\cdot}97 - e)^2}{1 + e}\sigma'^{0{\cdot}5} \tag{5}$$

where G_0 is in MPa and σ' in kPa. The comparison of calculated G_0 values with measured ones given in Fig. 14(b) indicates that Hardin's equation tends to overestimate G_0 values of the mixtures, particularly at a large confining stress and with a high fines content. It is to be mentioned that the comparison shown in Fig. 14 is not intended to claim that the proposed equation is superior to Hardin's equation; rather, it is to suggest that care should be exercised in the direct use of Hardin's equation for sand–fines mixtures.

MICROMECHANICAL CONSIDERATIONS

Exploring the underlying mechanism for the reduction of G_0 caused by the presence of fines is of considerable interest. The existing explanation seems to suggest that the fines in a sand–fines mixture are positioned in the voids formed by sand grains and do not develop effective contacts with sand grains (Salgado *et al.*, 2000). In other words, the fines act as voids rather than solids in a sand–fines mixture and accordingly the mixture will have a lower G_0 when compared with the base sand at the same void ratio. This explanation appears to follow the concept of the so-called skeleton or granular void ratio (Mitchell, 1976; Kuerbis *et al.*, 1988), which states that the void ratio of a sand–fines mixture is better quantified by a skeleton void ratio (e_s) rather than the usual void ratio (e) as

$$e_s = \frac{e + \mathrm{FC}}{1 - \mathrm{FC}} \tag{6}$$

where FC is fines content in decimal. With this density index, the consequence of inclusion of fines becomes an increase in the skeleton void ratio and thus a decrease in G_0 values.

The above concept was followed by Rahman *et al.* (2014) in formulating a constitutive model for sand–fines mixtures, in which they proposed that the empirical equation for clean sand can be directly used for sand–fines mixtures as long as the usual void ratio in the equation is replaced by the skeleton void ratio or its modified form. The validity of the proposal can be examined using the experimental data obtained from the current study. In doing so, an empirical equation is first established from RC test data on clean Toyoura sand as a reference

$$G_0\ (\mathrm{MPa}) = 95{\cdot}39\frac{(2{\cdot}17 - e)^2}{1 + e}\left(\frac{\sigma'}{p_a}\right)^{0{\cdot}37} \tag{7}$$

Then the G_0 values for Toyoura sand mixed with different quantities of silica fines are calculated by substituting e_s into equation (7). Fig. 15 shows the calculated G_0 values plotted against the measured ones. Evidently, the use of the skeleton void ratio significantly underestimates G_0 values of the mixtures even at a low percentage of fines (FC = 5% and 10%), and the discrepancy becomes larger as the quantity of fines increases. This indicates that the concept of the granular void ratio does not work well.

To explore the micro-scale mechanism of small-strain stiffness of granular materials, Gu & Yang (2013) conducted a series of numerical experiments on a regular packing of spheres with different diameter tolerances by using the discrete-element method (DEM). An important finding of their study is that, at an approximately constant void ratio, the G_0 of the packing increases as the coordination number increases (Fig. 16). In the context of micromechanics, the coordination number is a key index describing the arrangement of discrete particles in an assembly under a given confinement, and it is defined as the average contact number per particle. Drawing on this grain-scale analysis, it is hypothesised that the reduction of G_0 caused by the addition

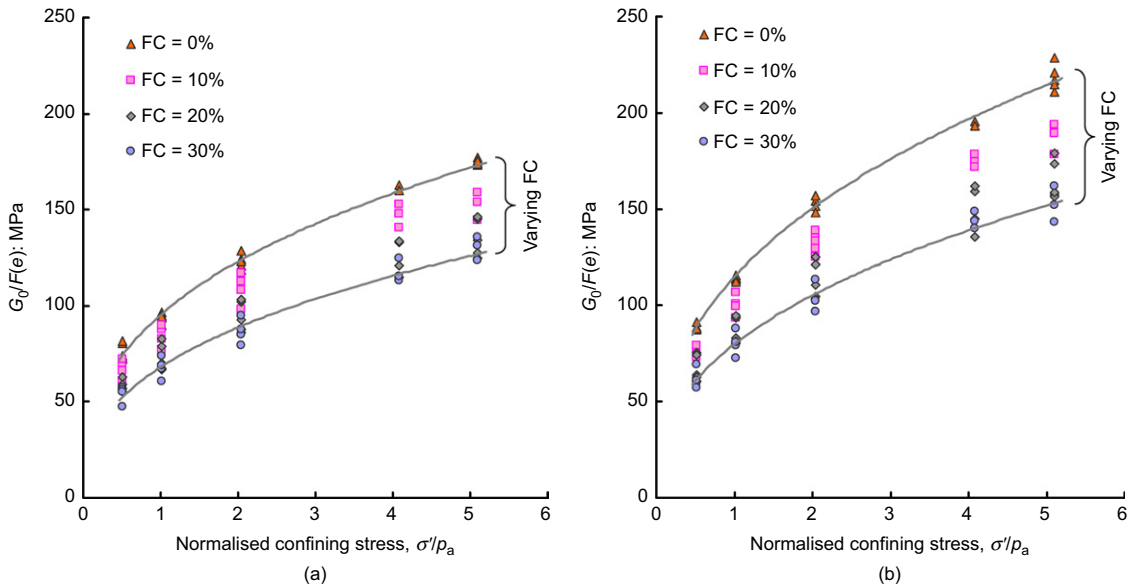

Fig. 12. Void ratio-corrected shear modulus as a function of normalised confining stress: (a) RC tests; (b) BE tests

Table 4. Best-fit parameters for shear modulus measurements

FC: %	Test method	Fitting parameters*		R^2
		A	n	
0	BE	114·38	0·38	1·00
	RC	95·39	0·37	0·99
5	BE	105·96	0·39	0·99
	RC	88·83	0·39	0·99
10	BE	100·52	0·40	0·99
	RC	85·92	0·37	0·96
20	BE	89·30	0·39	0·95
	RC	73·42	0·37	0·95
30	BE	85·89	0·40	0·97
	RC	68·14	0·38	0·96

*A (in MPa) and n are the two parameters in equation (1) with the void ratio function in equation (3).

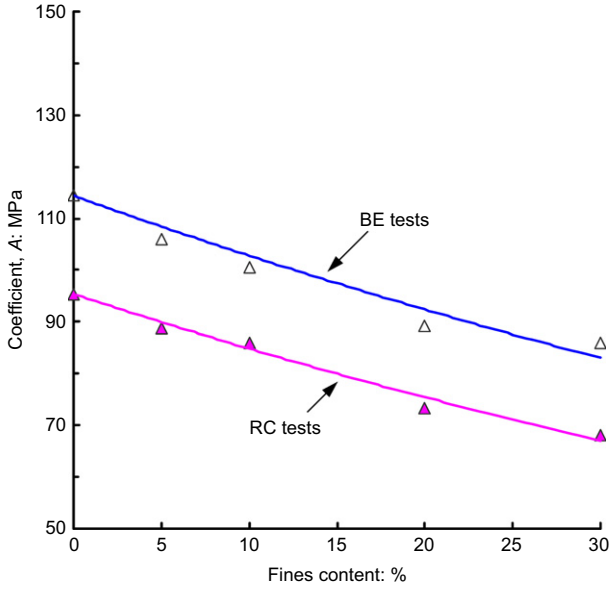

Fig. 13. Variation of coefficient A with fines content

of fines into clean sand, observed at an approximately constant void ratio, is mainly associated with the reduction in the coordination number. Note that this reduction in the coordination number differs from that associated with an increase in the void ratio (e.g. Chang *et al.*, 1991), which has been well recognised.

The hypothesis is schematically illustrated in Fig. 17, where three idealised packings are given to represent three cases: case (a), Fig. 17(a), is for clean sand without fines, case (b), Fig. 17(b), is for sand with a small amount of fines, and case (c), Fig. 17(c), for sand with a relatively large amount of fines. Note that all three packings have the same solid fraction and hence the same void ratio, but they possess different coordination numbers. For the clean sand case, the coordination number is the highest and hence its G_0 is the largest, whereas in case (c) the coordination number is the least and correspondingly its G_0 is the smallest. To verify the hypothesis about the effect of fines on the coordination number, a series of three-dimensional DEM simulations of random assemblies of spherical particles of coarse and fine sizes under triaxial loading have been conducted. In the simulations the mean size of coarse particles was set to be 1032 μm whereas the mean size of fine particles was set as 245 μm, giving the size ratio of 4·21. This ratio is comparable with that of Toyoura sand–fines mixtures (4, see Table 1). The simulation results, shown in Fig. 18, confirm that, at a given void ratio, the coordination number tends to decline as the quantity of fine particles increases, suggesting that the decrease in the coordination number is a sound micro-scale mechanism for the reduction of G_0 observed at the macro-scale. Note that in calculating the coordination number, particles with zero or only one contact have been excluded as they make no contribution to the stable state of stress (Thornton, 2000). Readers are referred to Luo & Yang (2013) where some additional interesting results were given.

UNIFIED CHARACTERISATION OF G_0

In the current literature, the common approach to characterising G_0 values for sand is to account separately for the influence of void ratio and confining stress, as for example expressed in equation (1). When fines are present in a clean sand, this empirical approach will lead to a set of trend curves in the $G_0/F(e)$–(σ'/p_a) plane, as shown in Fig. 12, with each curve corresponding to a mixture at a specific

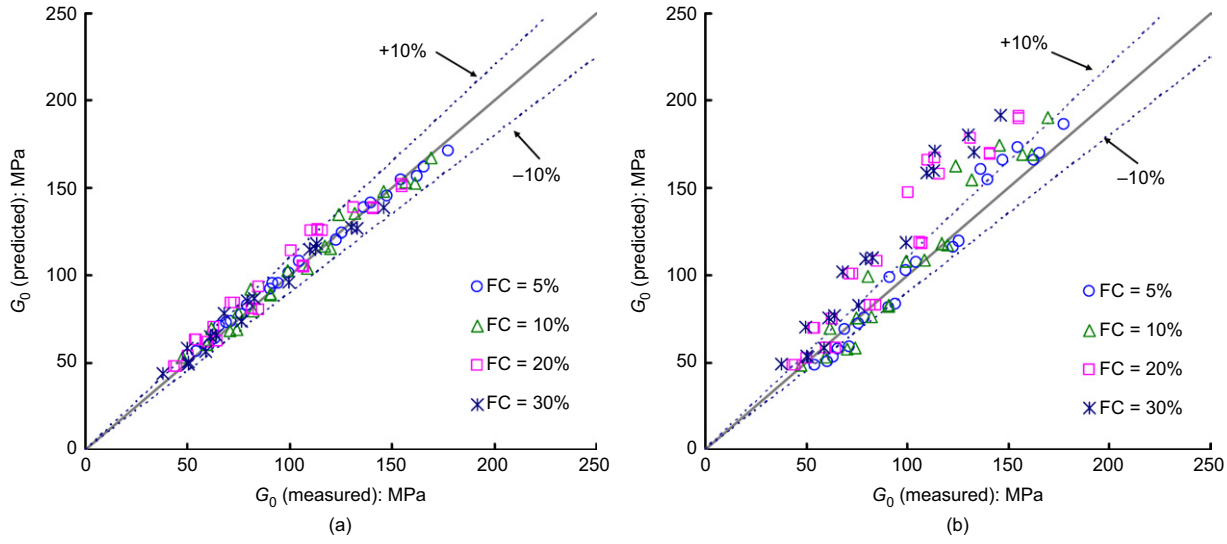

Fig. 14. Predicted plotted against measured shear modulus values: (a) proposed equation; (b) Hardin equation

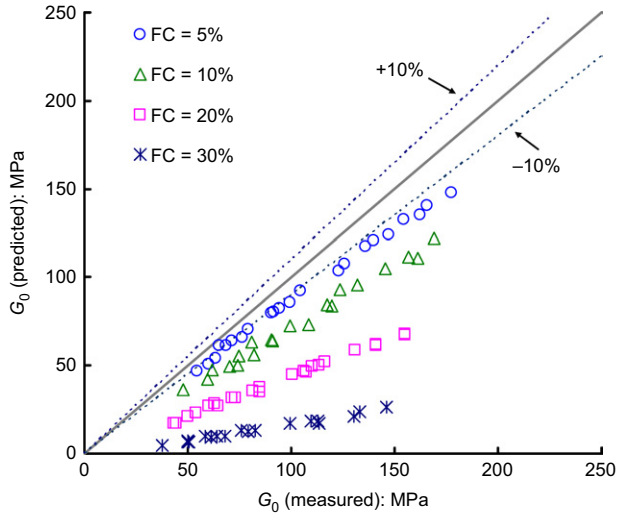

Fig. 15. Predicted shear modulus values using the concept of skeleton void ratio plotted against measured values

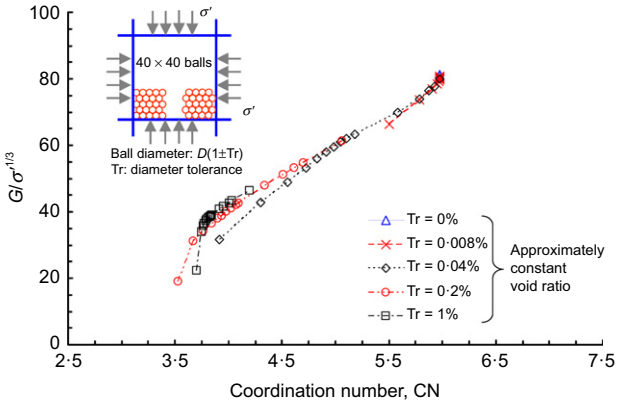

Fig. 16. Shear modulus as a function of coordination number at an approximately constant void ratio (after Gu & Yang, 2013)

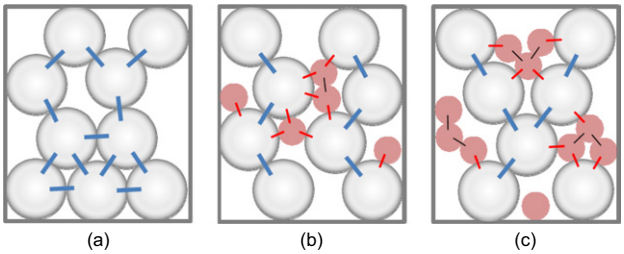

Fig. 17. Schematic illustration of particle contacts in packings at a constant void ratio: (a) clean sand without fines; (b) clean sand with a small amount of fines; (c) clean sand with a large amount of fines

percentage of fines. Exploring whether a unified characterisation of G_0 can be developed for both clean sand and its mixtures in a theoretical framework is of considerable interest.

In the study of the mechanical behaviour of sands with particular reference to the liquefaction phenomenon (e.g. Casagrande, 1971; Poulos *et al.*, 1985; Verdugo & Ishihara, 1996; Yang, 2002), it has been well recognised that various aspects of the behaviour can be characterised in the framework of critical state soil mechanics, which defines a unique critical state locus in the void ratio–mean effective stress (i.e. e–p') plane such that the locus serves as a boundary

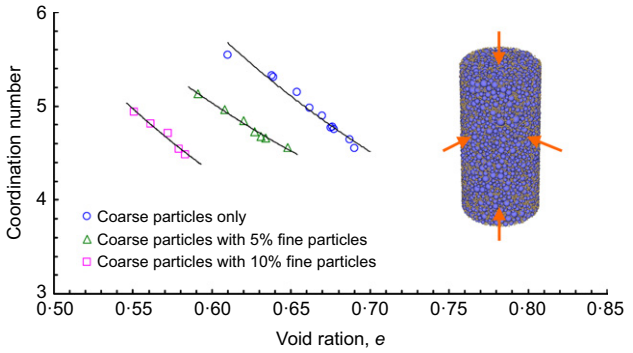

Fig. 18. Influence of fine particles on the coordination number of granular assemblies

separating the initial states of sand into contractive and dilative regions (Schofield & Wroth, 1968; Been & Jefferies, 1985; Wood, 1990). The nature of the critical state locus implies that the behaviour of sand can be more closely related to the proximity of its current state to the critical state locus. A state parameter (ψ), defined as the difference between the void ratio at the current state and the void ratio at the critical state under the same mean effective stress (Been & Jefferies, 1985), has been found useful in capturing various aspects of the stress–strain–strength behaviour of sand (e.g. Jefferies, 1993; Gajo & Wood, 1999; Yang & Li, 2004). Notably, a state parameter-based platform has also been established to analyse the cyclic strength of sand under both symmetric and non-symmetric loading conditions (Yang & Sze, 2011).

Hence, an attempt is made here to explore whether the state dependence of G_0 can be better characterised using this state parameter. The critical state loci of the mixtures (FC = 0, 5%, 10% and 20%) were carefully determined in the earlier study of Yang & Wei (2012), as shown in the four plots in Fig. 19. On each plot the states of the specimens tested in the current study are superimposed, showing a wide spectrum of states ranging from very loose to very dense with reference to the critical state.

For a given confining stress, say 100 kPa, the values of G_0 obtained from RC tests for specimens of clean sand and mixtures are presented as a function of the state parameter in Fig. 20(a). It is very encouraging to note that regardless of fines content, a unique trend line emerges that can fit all data points fairly well. Similar results are obtained for other cases of confining stress, as shown in Figs 20(b)–20(d). All these plots indicate that G_0 tends to decrease approximately linearly with an increasing state parameter, meaning that as the specimen becomes loose its G_0 reduces – this is certainly a reasonable trend.

Furthermore, by taking account of the stress dependence and introducing a state parameter function, $F(\psi)$, a general expression for characterising G_0 is proposed as follows

$$G_0 = A_\psi F(\psi)\left(\frac{\sigma'}{p_a}\right)^m = A_\psi \frac{(a-\psi)^2}{1+\psi}\left(\frac{\sigma'}{p_a}\right)^m \quad (8)$$

where A_ψ, a and m are parameters that can be determined by regression analysis. For example, using RC test data obtained for samples of FC = 0, 5%, 10% and 20%, the general expression in equation (8) can be further given as

$$G_0\ (\text{MPa}) = 41{\cdot}33\frac{(1{\cdot}36-\psi)^2}{1+\psi}\left(\frac{\sigma'}{p_a}\right)^{0{\cdot}4} \quad (9)$$

In Fig. 21 the experimental data points are plotted together with the trend line represented by equation (9) in the plane of $G_0/F(\psi)$–$(\sigma'/p_a)^{0{\cdot}4}$. A unified characterisation

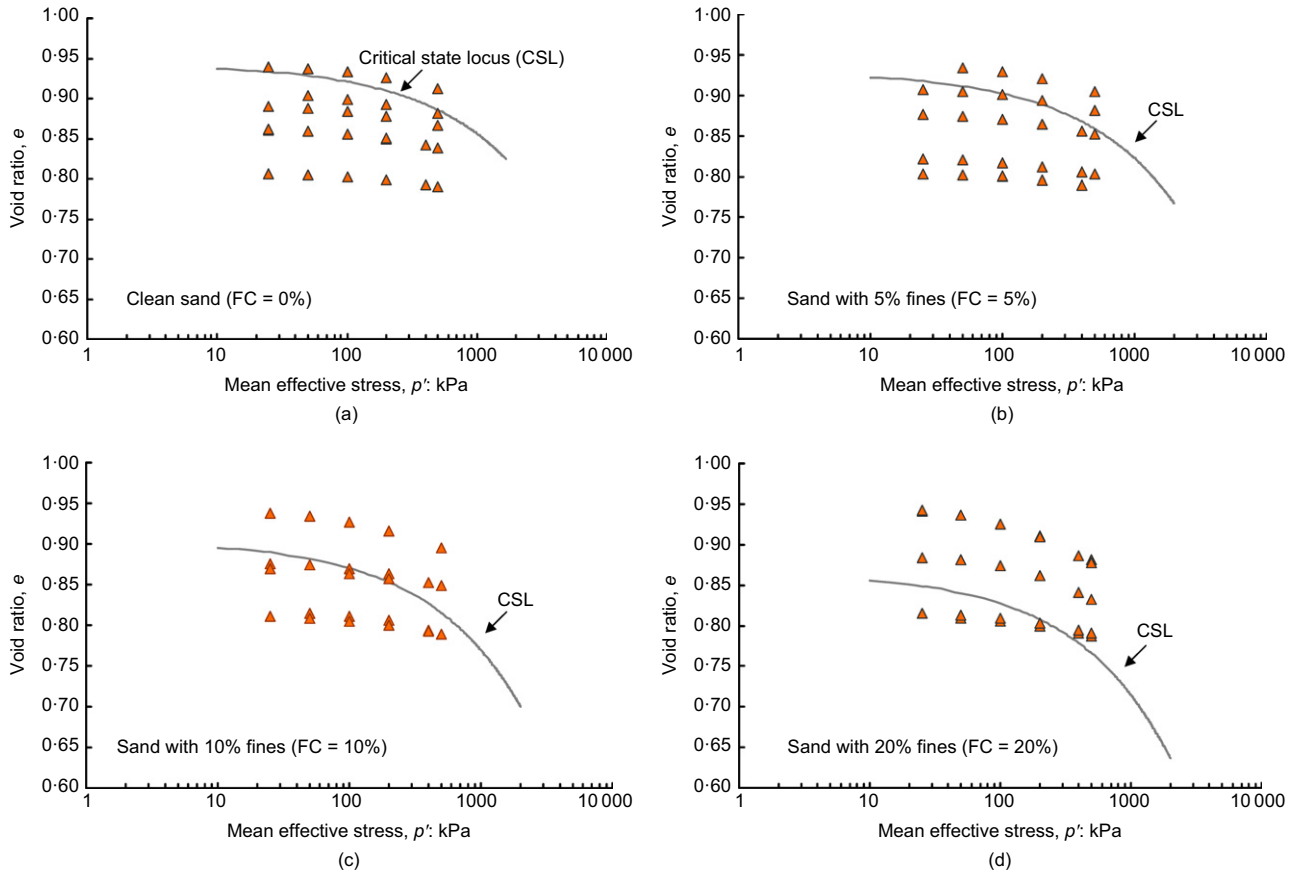

Fig. 19. States of specimens with reference to critical state locus: (a) FC = 0%; (b) FC = 5%; (c) FC = 10%; (d) FC = 20%

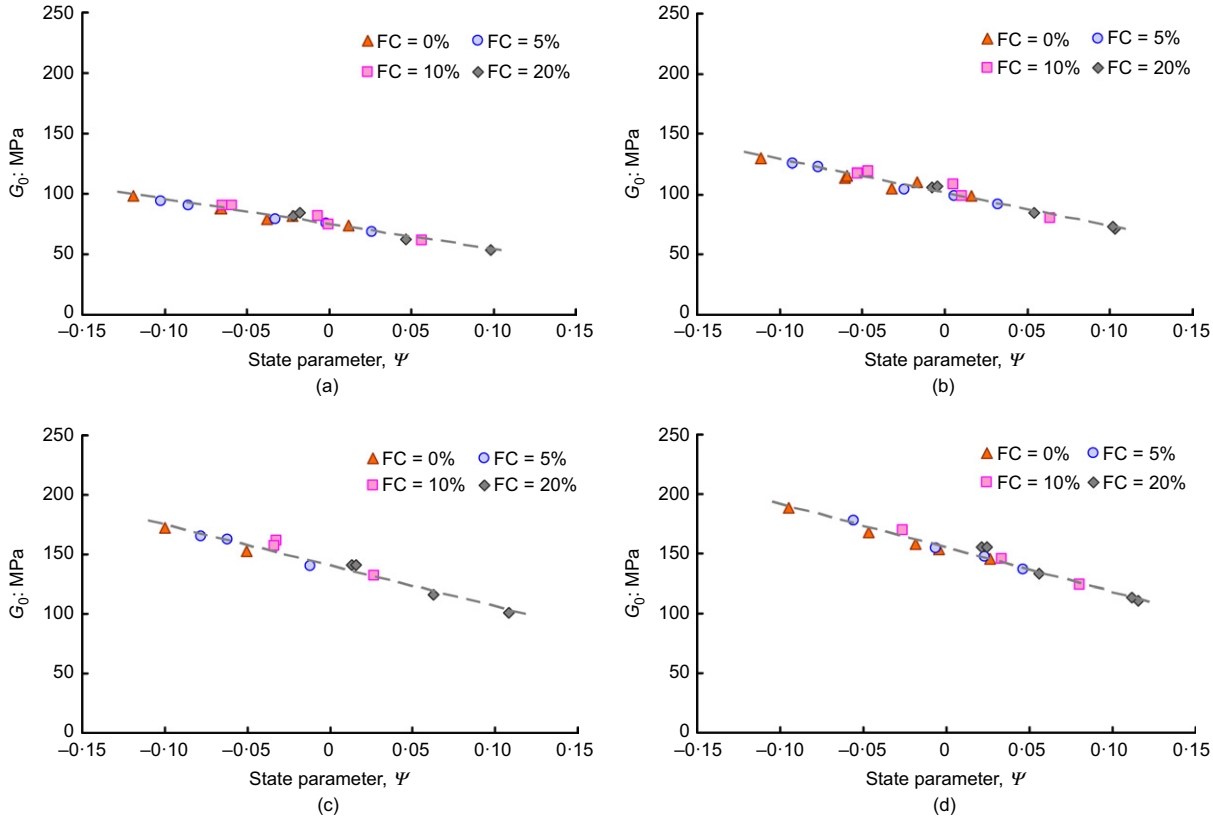

Fig. 20. Variation of shear modulus with state parameter at different confining stresses: (a) $\sigma' = 100$ kPa; (b) $\sigma' = 200$ kPa; (c) $\sigma' = 400$ kPa; (d) $\sigma' = 500$ kPa

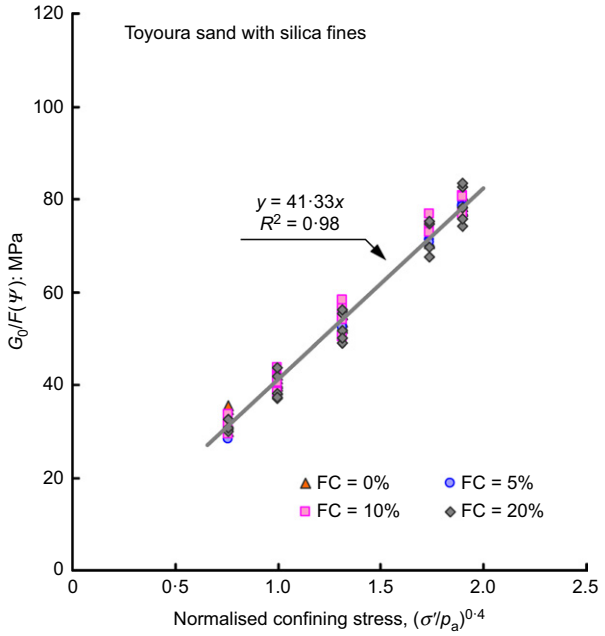

Fig. 21. State parameter-corrected shear modulus plotted against normalised confining stress

of G_0 values for both clean sand and sand–fines mixtures is achieved satisfactorily.

The general expression proposed in equation (8) is not trivial, but rather it is of significance in several aspects. First, it provides a rational approach for characterising the state-dependent G_0 in a unified way. Second, because it is anchored with the state parameter – which has been shown in previous studies to be useful in describing various aspects of the large-strain behaviour of granular soils – the expression provides theoretical insights into the various empirical methods that involve correlations between the small-strain stiffness property and the large-strain response, for example the shear wave-based method for liquefaction evaluation (Ishihara, 1996; Stokoe *et al.*, 1999).

Given the complexity of the effect of fines, further work to validate the unified approach by using experimental data on granular soils of varying size, shape and mineralogy is worthwhile. For gap-graded binary mixtures, the size ratio between coarse and fine grains has long been recognised as an important factor affecting soil behaviour such as piping (e.g. Skempton & Brogan, 1994; Shire *et al.*, 2014) and static liquefaction (Wei, 2012). An effort has thus been made to carry out similar testing series on mixtures of Fujian sand and crushed silica fines to examine the effect of size ratio on G_0. Compared with Toyoura sand, Fujian sand is also a uniform quartz sand with sub-angular to sub-rounded grains, but it has a larger mean size ($D_{10} = 282{\cdot}0$ μm, $D_{50} = 397$ μm, $C_u = 1{\cdot}532$), leading to mixtures with a larger size ratio (7·35). Fig. 22(a) shows G_0 values plotted against void ratios at three different percentages of fines (FC = 0, 5% and 10%), measured using the RC method under the confining pressure of 100 kPa. Similarly, at a given void ratio, G_0 declines as the quantities of fines increases; but the reduction rate appears to be larger than that for Toyoura sand, and this is thought to be mainly associated with the effect of size ratio. Using the critical state loci defined by Yang & Wei (2012) for mixtures of Fujian sand and silica fines and using ψ as the state variable, the three trend lines in Fig. 22(a) tend to merge into a single line regardless of fines content (Fig. 22(b)), showing that G_0 decreases with an increasing state parameter.

One more particular concern is whether the proposed approach works for natural silty sands with continuous grading. Experimental studies that contain adequate information for interpretation in this respect are lacking in the literature. Huang *et al.* (2004) reported test data on shear wave velocity (V_s) for a natural silty sand with different quantities of fines, measured at a confining pressure of 100 kPa by using bender elements installed in a triaxial device. They also conducted a series of monotonic loading tests leading to the information on critical states, but the V_s data were analysed using the conventional method of Hardin & Richart (1963). Fig. 23(a) shows the measured V_s data as a function of void ratio at different fines contents. For a given void ratio, V_s decreases with increasing fines content. By converting V_s to G_0 and then plotting the data against the calculated state parameters, it is very encouraging to notice that a unique trend line fitting all data points can be drawn, regardless of fines content, and the trend line also suggests a reduction of G_0 as the state parameter increases.

The state parameter-based approach appears to work reasonably well for both gap-graded and continuously graded mixtures. This finding should be expected since the approach is established in the critical state framework, with particular reference to the critical state locus in the compression space. As observed in many experimental studies, the critical state locus tends to change its position with changes in soil grain characteristics (e.g. gradation and particle shape), and this change will consequently lead to changes in the state parameter for a given void ratio and hence changes in G_0 and V_s.

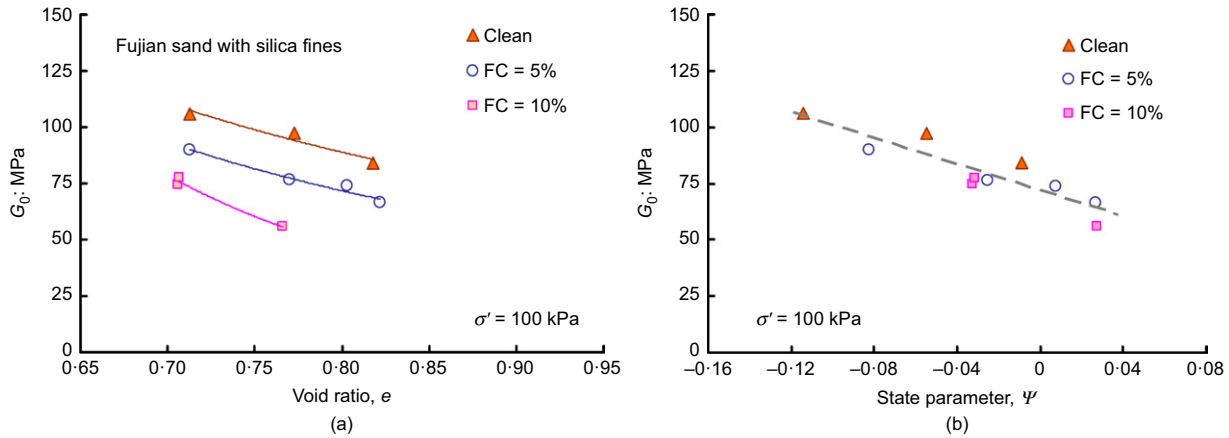

Fig. 22. RC test results for Fujian sand with fines: (a) G_0 plotted against void ratio; (b) G_0 plotted against state parameter

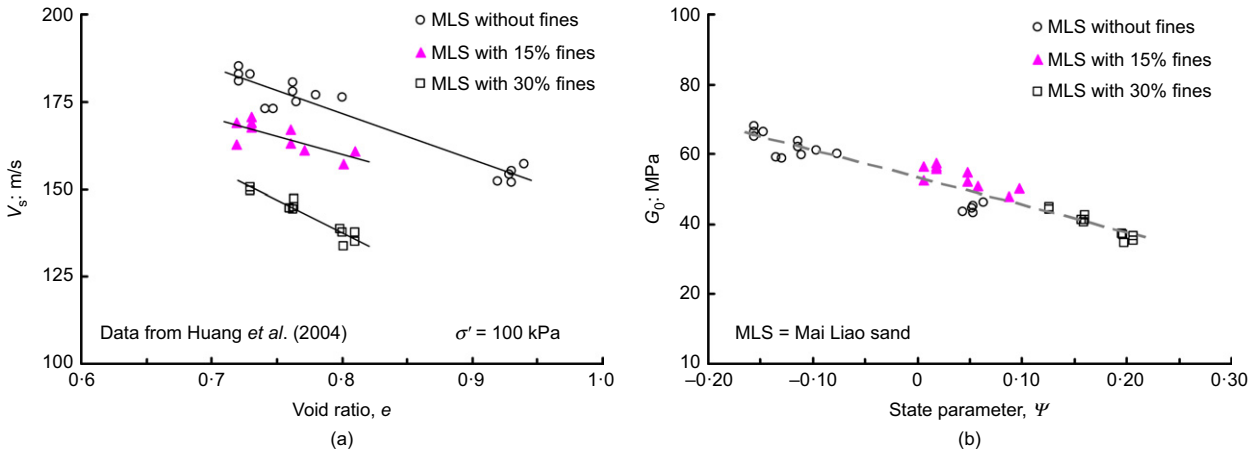

Fig. 23. Interpretation of test data on a natural silty sand with continuous grading: (a) measured shear wave velocity; (b) converted shear modulus as a function of state parameter

SUMMARY AND CONCLUSIONS

This paper presents a study where the aim was to investigate how the addition of fines alters the shear wave velocity (V_s) and associated stiffness (G_0) of sand through well-controlled laboratory experiments in conjunction with analysis and interpretation at the macro and micro scale. The main findings resulting from the study are summarised as follows.

(a) The RC and BE tests consistently show that for the range of fines content (0–30%) considered, the value of G_0 tends to decrease continuously as the quantity of fines is increased. By removing the influence of the void ratio, the rates of reduction due to the addition of fines appear to be similar and do not show a notable dependence on the confining stress.

(b) Both RC and BE tests yield a similar stress dependence for G_0 and the stress exponent does not appear to be sensitive to changes in fines content. The reduction of G_0 is mainly reflected by the coefficient A in the way that its value decreases exponentially with increasing fines content, and the size ratio between coarse and fine particles may play an important role in the variation of A with fines content.

(c) The effect of testing method on G_0 appears to be coupled with sample reconstitution methods or associated sample fabrics. For samples prepared by the moist tamping method, G_0 values measured by BE testing are notably greater than those measured by RC testing, whereas for samples prepared by the dry tamping method, the BE and RC measurements tend to become comparable.

(d) A new approach that allows the unified characterisation of G_0 values for both clean sand and sand–fines mixtures is established in the framework of critical state soil mechanics. Anchored with a state parameter with reference to the critical state locus, the approach provides important insights into the various empirical correlations that involve V_s or G_0 in geotechnical engineering practice.

(e) The micro-scale mechanism for the observed reduction of G_0 is considered to be associated with the decrease of the coordination number caused by the presence of fines at an approximately constant void ratio. The existing explanation that fines act as voids in a sand–fines mixture is shown to be unsupported by the experimental data.

(f) Given the simultaneous use of RC and BE techniques and the broad range of states covered, the experimental data sets provide a useful reference for the validation and calibration of numerical simulations and theoretical developments in the area. Future work towards validation of the unified approach using physical and/or numerical experiments on different materials is worthwhile.

ACKNOWLEDGEMENTS

The financial support provided by the Natural Science Foundation of China (NSFC) through the Overseas Investigator Award (no. 51428901) and by the University of Hong Kong through the Seed Funding for Basic Research scheme is gratefully acknowledged. The lead author is also thankful to Shanghai Jiao Tong University for the Distinguished Visiting Professorship during the course of this research.

NOTATION

A	coefficient in equation (1)
A_ψ	coefficient in equation (8)
a	parameter in equation (8)
C_u	coefficient of uniformity
D_{10}	grain size at which 10% of sample is finer
D_{50}	mean particle size
D_{60}	grain size at which 60% of sample is finer
e	void ratio after consolidation
e_s	skeleton void ratio
$F(e)$	void ratio function
$F(\psi)$	state parameter function
f_{in}	frequency of input signal in BE test
f_n	resonant frequency
G_0	small-strain shear stiffness
G_s	specific gravity
I	mass polar moment of inertia of specimen
I_0	mass polar moment of inertia of added mass
L	height of specimen
m, n	stress exponents
p'	mean effective stress
p_a	reference stress
q	deviatoric stress
V_s	shear wave velocity
β	parameter in equation (2)
ε_a	axial strain
σ'	mean effective stress
ψ	state parameter

REFERENCES

Been, K. & Jefferies, M. G. (1985). A state parameter for sands. *Géotechnique* **35**, No. 2, 99–102, http://dx.doi.org/10.1680/geot.1985.35.2.99.

Brignoli, E. G. M., Gotti, M. & Stokoe, K. H. II (1996). Measurement of shear waves in laboratory specimens by means of piezoelectric transducers. *Geotech. Test. J.* **19**, No. 4, 384–397.

Casagrande, A. (1971). On liquefaction phenomena. *Géotechnique* **21**, No. 3, 197–202, http://dx.doi.org/10.1680/geot.1971.21.3.197.

Chang, C. S., Misra, A. & Sundaram, S. S. (1991). Properties of granular packing under low amplitude cyclic loading. *Soil Dynam. Earthquake Engng* **10**, No. 4, 201–211.

Chien, L. K. & Oh, Y. N. (2002). Influence of fines content and initial shear stress on dynamic properties of hydraulic reclaimed soil. *Can. Geotech. J.* **39**, No. 1, 242–253.

Clayton, C. R. I. (2011). Stiffness at small-strain: research and practice. *Géotechnique* **61**, No. 1, 5–38, http://dx.doi.org/10.1680/geot.2011.61.1.5.

Gajo, A. & Wood, D. M. (1999). Severn–Trent sand: a kinematic-hardening constitutive model: the *q–p* formulation. *Géotechnique* **49**, No. 5, 595–614, http://dx.doi.org/10.1680/geot.1999.49.5.595.

Goddard, J. D. (1990). Nonlinear elasticity and pressure-dependent wave speeds in granular media. *Proc. R. Soc. London* **430**, No. 1878, 105–131.

Gu, X. Q. & Yang, J. (2013). A discrete element analysis of elastic properties of granular materials. *Granular Matter* **15**, No. 2, 139–147.

Gu, X. Q., Yang, J., Huang, M. S. & Gao, G. Y. (2015). Bender element tests in dry and saturated sand: signal interpretation and result comparison. *Soils Found.* **55**, No. 5, 951–962.

Hardin, B. O. & Black, W. L. (1966). Sand stiffness under various triaxial stresses. *J. Soil Mech. Found. Div. ASCE* **92**, No. SM2, 27–42.

Hardin, B. O. & Drnevich, V. P. (1972). Shear modulus and damping in soil: Design equation and curves. *J. Soil Mech. Found. Div., ASCE* **98**, No. 7, 667–692.

Hardin, B. O. & Richart, F. E. (1963). Elastic wave velocities in granular soils. *J. Soil Mech. Found. Div., ASCE* **89**, No. SM1, 39–56.

Hicher, P. Y. (1996). Elastic properties of soils. *J. Geotech. Engng, ASCE* **122**, No. 8, 641–648.

Huang, Y. T., Huang, A. B., Kuo, Y. C. & Tsai, M. D. (2004). A laboratory study on the undrained strength of a silty sand from Central Western Taiwan. *Soil Dynam. Earthquake Engng* **24**, 733–743.

Ishihara, K. (1996). *Soil behaviour in earthquake geotechnics*. Oxford, UK: Clarendon Press.

Iwasaki, T. & Tatsuoka, F. (1977). Effect of grain size and grading on dynamic shear moduli of sand. *Soils Found.* **17**, No. 3, 19–35.

Jefferies, M. G. (1993). Nor-Sand: a simple critical state model for sand. *Géotechnique* **43**, No. 1, 93–103, http://dx.doi.org/10.1680/geot.1993.43.1.91.

Jovicic, V., Coop, M. R. & Simic, M. (1996). Objective criteria for determining G_{max} from bender element tests. *Géotechnique* **46**, No. 2, 357–362, http://dx.doi.org/10.1680/geot.1996.46.2.357.

Kuerbis, R., Negussey, D. & Vaid, Y. P. (1988). Effect of gradation and fines content on the undrained response of sand. In *Hydraulic fill structures* (ed. D. J. A. Van Zyl), Geotechnical Special Publication No. 21, pp, 330–345. Reston, VA, USA: American Society of Civil Engineers.

Kuwano, R., Connolly, T. M. & Jardine, R. J. (2000). Anisotropic stiffness measurements in a stress-path triaxial cell. *Geotech. Testing J.* **23**, No. 2, 141–157.

Ladd, R. S. (1978) Preparing specimens using undercompaction. *Geotech. Testing J.* **1**, No. 1, 16–23.

Lade, P. V. & Yamamuro, J. A. (1997). Effect of non-plastic fines on static liquefaction on sands. *Can. Geotech. J.* **34**, No. 6, 918–928.

Lee, J. & Santamarina, J. C. (2005). Bender elements: performance and signal interpretation. *J. Geotech. Geoenviron. Engng, ASCE* **131**, No. 9, 1063–1070.

Lo Presti, D. C. F., Jamiolkowski, M., Pallara, O., Cavallaro, A. & Pedroni, S. (1997). Shear modulus and damping of soils. *Géotechnique* **47**, No. 3, 603–617, http://dx.doi.org/10.1680/geot.1997.47.3.603.

Luo, X. D. & Yang, J. (2013). Effects of fines on shear behavior of sand: a DEM analysis. In *Proceedings of 5th international young geotechnical engineers' conference* (eds Y.-J. Cui, F. Emeriault and F. Cuira), pp. 265–268. Paris, France: IOS Press.

McDowell, G. R. & Bolton, M. D. (2001). Micro mechanics of elastic soil. *Soils Found.* **41**, No. 6, 147–152.

Mitchell, J. K. (1976). *Fundamentals of soil behavior*. Hoboken, NJ, USA: John Wiley & Sons.

Miura, S. & Toki, S. (1982). A sample preparation method and its effect on static and cyclic deformation strength properties of sand. *Soils Found.* **22**, No. 1, 61–77.

Nakagawa, K., Soga, K. & Mitchell, J. K. (1997). Observation of Biot compressional wave of the second kind in granular soils. *Géotechnique* **47**, No. 1, 133–147, http://dx.doi.org/10.1680/geot.1997.47.1.133.

Polito, C. & Martin, J. (2001). Effects of non-plastic fines on the liquefaction resistance of sands. *J. Geotech. Geoenviron. Engng, ASCE* **127**, No. 5, 408–415.

Poulos, S. J., Castro, G. & France, J. W. (1985). Liquefaction evaluation procedure. *J. Geotech. Engng Div., ASCE* **111**, No. 6, 772–792.

Rahman, M. M., Lo, S. R. & Dafalias, Y. F. (2014). Modelling the static liquefaction of sand with low-plasticity fines. *Géotechnique* **64**, No. 11, 881–894, http://dx.doi.org/10.1680/geot.14.P.079.

Salgado, R., Bandini, P. & Karim, A. (2000). Shear strength and stiffness of silty sand. *J. Geotech. Geoenviron. Engng, ASCE* **126**, No. 5, 451–462.

Schofield, A. N. & Wroth, C. P. (1968). *Critical state soil mechanics*. London, UK: McGraw-Hill.

Seed, H. B., Wong, R. T., Idriss, I. M. & Tokimatsu, K. (1986). Moduli and damping factors for dynamic analyses of cohesionless soil. *J. Geotech. Engng, ASCE* **112**, No. 11, 1016–1032.

Shire, T., O'Sullivan, C., Hanley, K. J. & Fannin, R. J. (2014). Fabric and effective stress distribution in internally unstable soils. *J. Geotech. Geoenviron. Engng, ASCE* **140**, No. 12, 04014072.

Skempton, A. W. & Brogan, J. M. (1994). Experiments on piping in sandy gravels. *Géotechnique* **44**, No. 3, 449–460, http://dx.doi.org/10.1680/geot.1994.44.3.449.

Stokoe, K. H., Darendeli, M. B., Andrus, R. D. & Brown, L. T. (1999). Dynamic soil properties: laboratory, field and correlation studies. In *Proceedings of 2nd international conference on earthquake geotechnical engineering*, pp. 811–845. Rotterdam, the Netherlands: Balkema.

Sze, H. Y. & Yang, J. (2014). Failure modes of sand in undrained cyclic loading: Impact of sample preparation. *J. Geotech. Geoenviron. Engng, ASCE* **140**, No. 1, 152–169.

Taiebat, M. & Dafalias, Y. F. (2008). Sanisand: simple anisotropic sand plasticity model. *Int. J. Numer. Analyt. Methods Geomech.* **32**, No. 8, 915–948.

Thevanayagam, S., Shenthan, T., Mohan, S. & Liang, J. (2002). Undrained fragility of clean sands, silty sands, and sandy silts. *J. Geotech. Geoenviron. Engng, ASCE* **128**, No. 10, 849–859.

Thornton, C. (2000). Numerical simulations of deviatoric shear deformation of granular media. *Géotechnique* **50**, No. 1, 43–53, http://dx.doi.org/10.1680/geot.2000.50.1.43.

Verdugo, R. & Ishihara, K. (1996). The steady state of sandy soils. *Soils Found.* **36**, No. 2, 81–91.

Wei, L. M. (2012). *Static liquefaction and flow failure of sandy soils*. PhD thesis, The University of Hong Kong, Pokfulam, Hong Kong.

Wichtmann, T. & Triantafyllidis, T. (2009). Influence of the grain-size distribution curve of quartz sand on the small-strain shear modulus G_{max}. *J. Geotech. Geoenviron. Engng, ASCE* **135**, No. 10, 1404–1418.

Wichtmann, T., Hernandez, M. & Triantafyllidis, T. (2015). On the influence of a non-cohesive fines content on small strain stiffness, modulus degradation and damping of quartz sand. *Soil Dynam. Earthquake Engng* **69**, 103–114.

Wood, D. M. (1990). *Soil behaviour and critical state soil mechanics*. Cambridge, UK: Cambridge University Press.

Yamashita, S., Kawaguchi, T., Nakata, Y., Mikami, T., Fujiwara, T. & Shibuya, S. (2009). Interpretation of international parallel test on the measurement of G_{max} using bender elements. *Soils Found.* **49**, No. 4, 631–650.

Yang, J. (2002). Non-uniqueness of flow liquefaction line for loose sand. *Géotechnique* **52**, No. 10, 757–760, http://dx.doi.org/10.1680/geot.2002.52.10.757.

Yang, J. & Gu, X. Q. (2013). Shear stiffness of granular material at small-strain: does it depend on grain size? *Géotechnique* **63**, No. 2, 165–179, http://dx.doi.org/10.1680/geot.11.P.083.

Yang, J. & Li, X. S. (2004). State-dependent strength of sands from the perspective of unified modeling. *J. Geotech. Geoenviron. Engng, ASCE* **130**, No. 2, 186–198.

Yang, J. & Sze, H. Y. (2011). Cyclic strength of sand under sustained shear stress. *J. Geotech. Geoenviron. Engng, ASCE* **137**, No. 12, 1275–1285.

Yang, J. & Wei, L. M. (2012). Collapse of loose sand with the addition of fines: the role of particle shape. *Géotechnique* **62**, No. 12, 1111–1125, http://dx.doi.org/10.1680/geot.11.P.062.

Youn, J. U., Choo, Y. W. & Kim, D. S. (2008). Measurement of small-strain shear modulus G_{max} of dry and saturated sands by bender element, resonant column, and torsional shear tests. *Can. Geotech. J.* **45**, No. 10, 1426–1438.